Crack detection method applied to 3D computed tomography images of baked carbon anode

Donald Picard[1], Julien Lauzon-Gauthier[2], Carl Duchesne[3], Houshang Alamdari[4], Mario Fafard[5], Donald Ziegler[6]

1. Research Engineer,
2. PhD Student,
3. Professor,
4. Professor,
5. Professor,

NSERC/Alcoa Industrial Research Chair MACE3 and Aluminium Research Centre – REGAL
Université Laval, Québec, QC, Canada

6. Program Manager – Modeling, Alcoa Primary Metals, Alcoa Technical Center, PA, USA

Corresponding author: Donald.Picard@gci.ulaval.ca

Abstract

Carbon anodes used in the aluminium industry have been investigated through destructive and non-destructive testing (NDT). In the latter case, computed tomography (CT) has been previously used to map the 3D apparent density distribution and is now extended to crack detection. Previous work has shown how to overcome technical hurdles related with crack detection by using percolation based algorithms operating on low resolution images of full-scale baked carbon anode. The previous application to 2D images is extended here to the 3D case. The crack detection algorithm has been performed on two inch thick anode slices containing several independent macro cracks. The influence of the cracks on other NDT techniques is also highlighted.

Keywords: Carbon anodes, computed tomography, crack detection, percolation algorithm.

1. General

Of all materials used in the electrolysis cell, only carbon anodes (approximately 30 anodes per cell) could be considered as consumable items requiring regular replacement. These anodes are consumed during electrolysis and replaced after approximately 26 days of operation. Depending of the cell technology, approximately one anode per cell is replaced each day. Hence a large number of anodes and consequently a large quantity of raw materials are required to operate a plant. Also, to stay economically competitive and considering the large amount of anodes consumed each year, aluminium producers need to reduce the cost of their anode production. Part of the solution is to reduce the cost of the raw materials. The drawback is that producers now have to deal with continuous changing of raw materials properties, resulting in a wide variation of physical properties of the baked anodes.

One solution to minimize the effect of the variation of raw materials properties is to use numerical simulation methods to model the manufacturing process and/or to increasing the process control. The objective is to predict the anode characteristics, to control the process parameters more efficiently and to take corrective actions before the anode is produced. To achieve this goal, a series of experimental data must be first collected in order to validate the models. From a density point of view, the most efficient way to get 3D information is through the use of computed tomography (CT). Non-destructive anode investigation had thus three main objectives: 1) to obtain the apparent density distribution, 2) to estimate the porosity distribution and 3) to quantify the larger cracks inside the anodes [1]. The anode density mapping has

already been addressed in previous studies [2, 3]. Hence, this paper focuses only on the quantification of large cracks in 3D.

1.1. X-ray computed tomography

Carbon anode images have been obtained by scanning a whole baked anode block using computed tomography (3D NDT imaging tool). The block investigated in this paper is the same one used in previous NDT studies [2-4]. The CT method has mainly one advantage that overcomes two disadvantages. The advantage is the nature of the technique itself, i.e. it is a non-destructive technique that does not involve the damaging or destruction of the sample and thus preserves crack integrity within the object. On the other hand, the scanning area of the X-ray apparatus (Siemens Somatom Sensation 64) was designed for the human body and consequently was too small for the anode (Figure 1). The block was thus sliced in 52 pieces of 50 mm thick [4] as illustrated in Figure 2. Also, to avoid excessive data, image resolution had to be adapted to the object size [4] resulting in a voxel (volumetric pixel) resolution of 0.7 × 0.6 × 0.7 mm^3 (the thickness of voxels is 0.7 mm). Assuming this resolution, a typical anode slice will contain approximately 70 × 468 × 1068 voxels (□ 35M voxels). Therefore, contrast between cracks and background (carbon) is reduced.

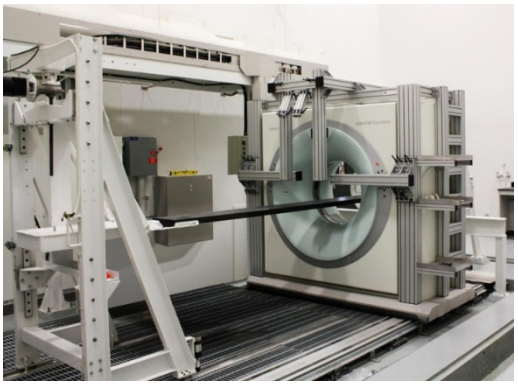

Figure 1 Siemens Somatom Sensation 64. Courtesy of INRS-ETE.

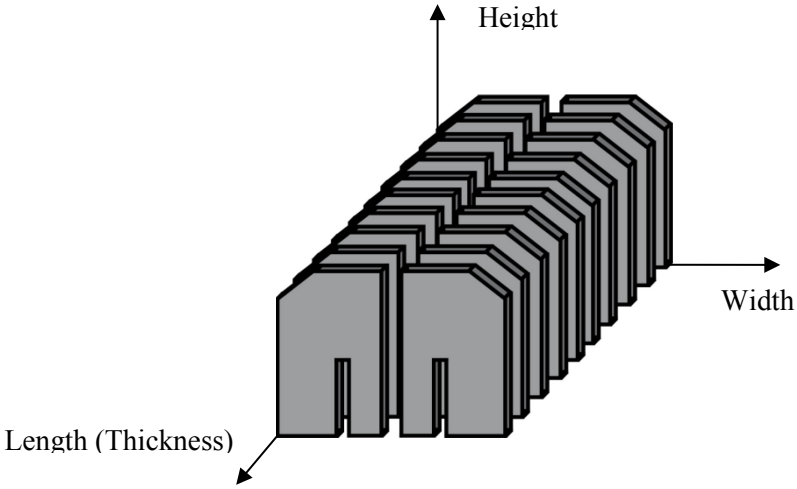

Figure 2 Scheme of the investigated anode slice pattern.

2. Crack detection method

Several image processing techniques are available for crack detection and have been summarized in [5]. Some focus on accuracy while others focus on decreasing computation time. However, most techniques have been developed for 2D. This could be explain by the complexity of three-dimensional morphological analysis of the region of interest (ROI) [6]. One of the criteria used for 3D crack detection is based on template matching [6, 7].

In the present study, the crack detection is based on the liquid permeation model, namely the percolation method (region growing method based on image segmentation). This method has recently been improved [5, 8-10] for 2D analysis and applied to low resolution anode material images [4]. The advantage of this method for low resolution images has already been highlighted in [4]. An extension of this model to 3D analysis is thus proposed in this paper. Before introducing the 3D extension, a summary of the 2D percolation is presented. A more detailed review of the 2D algorithm is available in [4, 10].

2.1. 2D algorithm

The improved 2D percolation algorithm [5, 8-10] is schematized in Figure 3. The definition of all parameters can be found in [10]. The proposed algorithm is a two steps analysis for each pixel candidate (seed pixel located in crack or pore) obtained through a pre-processing analysis [4, 5]. In the first step, percolation is performed until it reaches the boundary of a predetermined investigation window ($N \times N$ pixels). If the geometrical constraint is satisfied (i.e. circularity or roundness of the percolated region less than a specified threshold F_c), the percolation moves to the second step. The second phase of the algorithm consists of increasing incrementally the investigation window size up to a maximum size of $M \times M$ pixels or until the circularity reaches the threshold. In any case, only percolated region with a circularity less than the specified threshold will be identified as a crack.

2.2. 3D algorithm

The 3D algorithm developed in Matlab® is a direct extension of the 2D algorithm shown in Figure 3. To extend the 2D algorithm to the 3D case three challenges had to be overcome. The first one was to apply the percolation by inspecting the 3D neighbor voxels (26 neighbor for each voxel) of all the voxels included in the ROI (D_p) instead of the 2D neighbor pixels (8 neighbor for each pixel). This part was relatively straightforward. The second one is to define an investigation box (3D) instead of a window (2D). The box faces (or window sides) are used to define the boundary voxels that will stop processing when the percolation reaches those voxels. As for the window, the box dimensions must be representative of the typical crack length [10]. The box must also be able to adapt to the case study. In the present case, samples are anode slices with a thickness of 50 mm (approximately 80 voxels). Moreover, cracks are parallel to the length axis (also corresponding to thickness axis) and are, in most case, much longer than the slice thickness (i.e. most cracks propagate through 3 to 4 anode slices). The investigation box thus proposed is shown in Figure 4. When the slice thickness is smaller than the investigation box, the voxels of the dark faces of the box shown in Figure 4b are removed from the boundary voxels to avoid the end of the process prematurely. Similarly to the 2D percolation process, the investigation box dimensions will increase iteratively in the second phase, e.g. $N \times N \times N \rightarrow (N+2) \times (N+2) \times (N+2)$. The flowchart shown in Figure 4 is also applied during the iteration process.

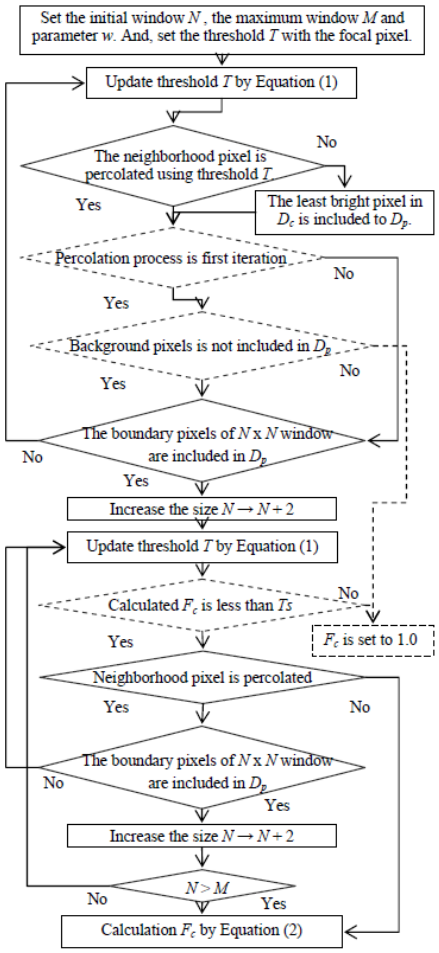

Figure 3 Flowchart of the percolation method [10].

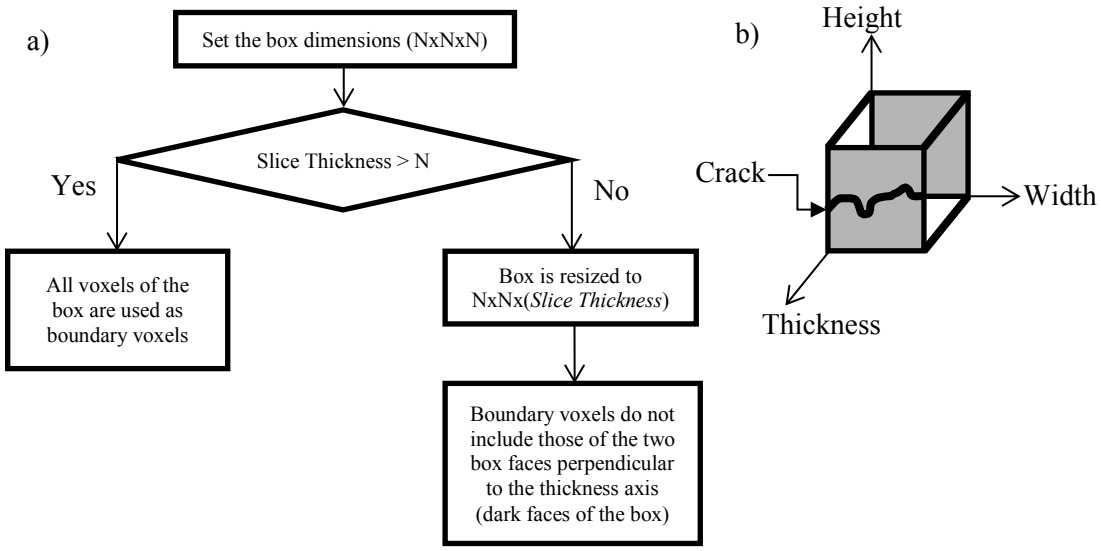

Figure 4 Flowchart for investigation box size determination: a) flowchart, b) investigation box.

The last challenge was to define a relevant 3D crack criterion (e.g. circularity in 2D). A three-dimensional object can be classified using several morphological features [7, 11]. At this stage, it is however unnecessary to do so. Only a threshold value of a defined parameter is needed to

distinguish a crack from a pore (or any other structures). The parameter chosen was the sphericity Ψ (Eq. (1)). It is defined as the ratio of the surface area of a sphere (with the same volume V_p as the given ROI) to the surface area (A_p) of the ROI [12]. In the present case, anode macro cracks are relatively thin compare to their length and width. Hence, the sphericity was a sufficient criterion for the 3D algorithm.

$$\Psi = \frac{\pi^{1/3}(6\,V_p)^{2/3}}{A_p} \tag{1}$$

3. Results

3.1. Pre-processing

In order to reduce computation time, it is preferable to define the candidate voxels or seed voxels (starting voxels for the percolation method) [10] instead of performing the percolation on each voxel in the 3D volume. In the present case, the same method used in the 2D analysis [4], i.e. a non-decimated wavelet transform (NDWT), has been used to identify the seed voxels within the 3D volume (anode slice). In a typical anode slice (70 × 468 × 1068 voxels with a resolution of 0.7 × 0.6 × 0.7 mm^3), after filtering the NDWT results [4], approximately 10 000 voxels (0.03 %) are tagged as seed voxels. However, not all seed voxels will initiate a percolation process since some of them will have been included in the ROI (D_p) of a previous percolation analysis. The result of pre-processing for a typical anode slice is shown in Figure 5. It is difficult to distinguish seed voxels located in cracks from those located in pores. Hence Figure 6 shows the seed voxels at half-width, i.e. for only one image.

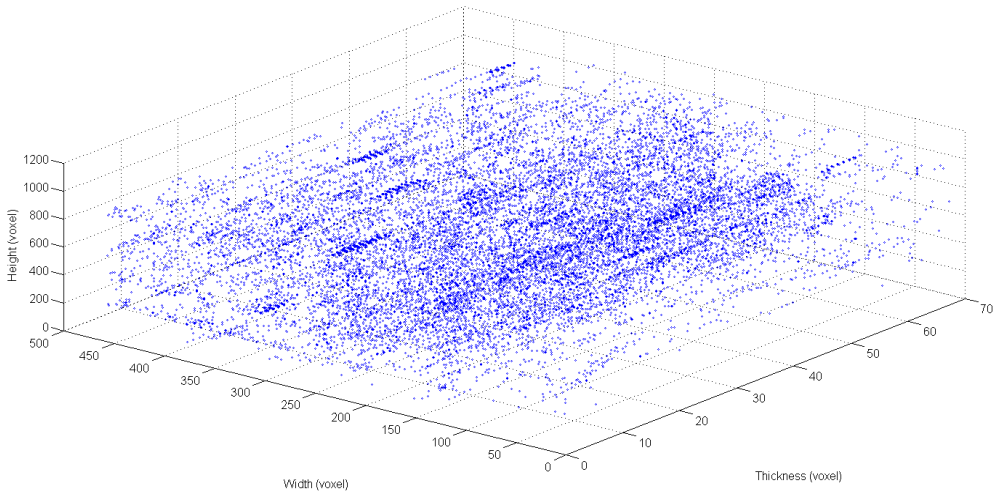

Figure 5 Seed voxels of a typical anode slice containing cracks and pores.

a)

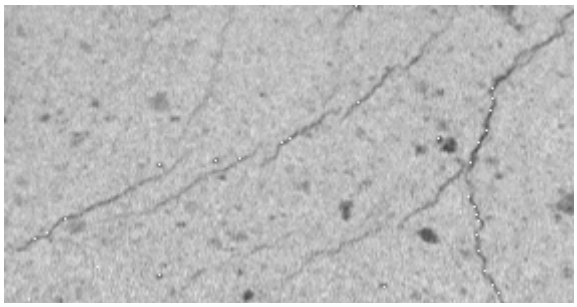

b)

Figure 6 Seed voxels (white pixels) of a typical anode image (center of the slice) containing cracks and pores. a) full scale. b) image zoomed in the region containing most cracks.

3.2. 3D Percolation

Two seed voxels located in cracks having two different sizes and morphologies, shown in Figure 7, have been used to show the performance of the 3D percolation algorithm. The algorithm is not yet optimized from a computation time point of view. Hence only the percolation result is analyzed. The first seed voxel is located near an anode slot and the second one close to an anode stub hole. As seen in that figure, cracks have a width of approximately 2 to 3 voxels and seem, form a 2D point of view, to be discontinuous.

a) 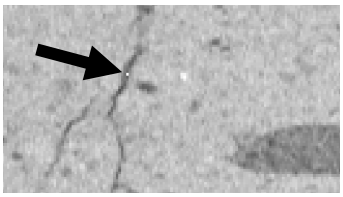

b) 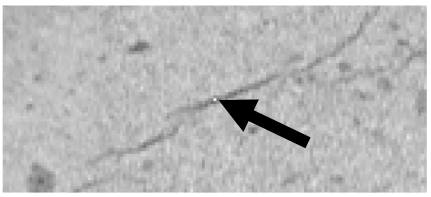

Figure 7 Selected seeds voxels (white) for 3D percolation process. a) Seed voxel #1. b) Seed voxel #2.

Also, the 3D Percolation process has been used with and without the boundary voxels of the dark faces of the investigation box shown in Figure 4. The sphericity threshold has been set to $\Psi = 0.5$. Figure 8 and Figure 9 shows the crack detection results on both seed voxels by using an investigation box (100 × 100 × 100 voxels) containing all boundary voxels (including the

voxels of the dark faces of Figure 4b). In the first case (seed voxel #1), the percolation process lead to a crack containing 2078 voxels. In the second case, 1367 voxels were identified. Compare to 2D percolation results [4] the 3D algorithm without constraint on the investigation box did not performed well (Figure 9).

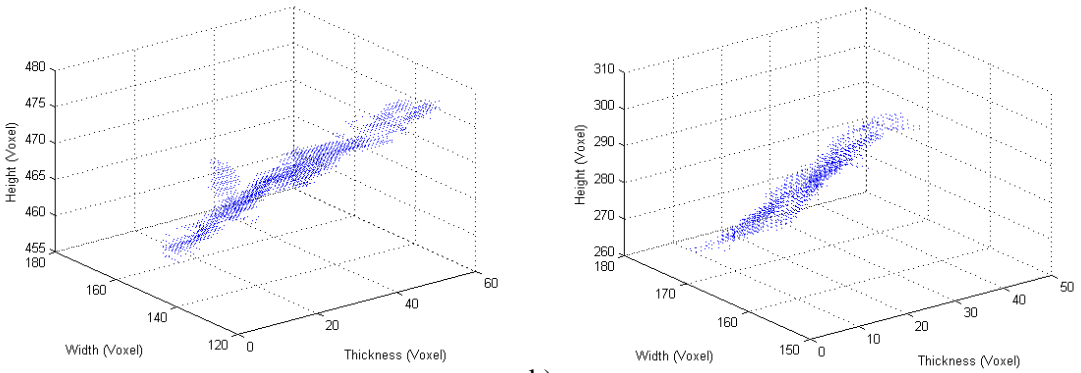

a) b)

Figure 8 Cracks detection results without restriction on the investigation box ($\Psi = 0.5$). a) Seed voxel #1. b) Seed voxel #2.

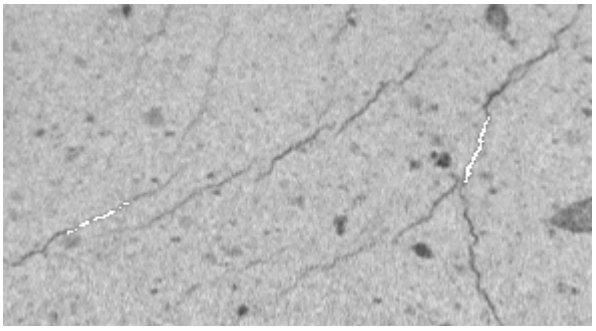

Figure 9 Cracks detection results (white regions) without restriction on the investigation box. Image located at mid width of the anode slice. Left crack: near stub hole. Right crack: near anode slot.

The used of a constrained investigation box (i.e. using the flowchart of Figure 4) on the selected seed voxels led to the results shown in Figure 10 and Figure 11. 6243 voxels were identified as part of the crack in the first case (seed voxel #1) and 17832 in the second one (seed voxel #2). A third crack seems to have been identified in Figure 11. However, the percolation process identified a volume where all identified voxels are connected, as shown in Figure 10a. Hence, both cracks on the left end of Figure 11 are part of the same 3D crack (percolated region related to seed voxel #2). The 3D algorithm has performed well in the second case (seed voxel #2), i.e. most voxels of the cracks have been identified. While the algorithm seems to have also performed well for the first seed voxels (Figure 10b), some parts of the cracks have been missed (right end of Figure 11). This is mainly related to the image low resolution limitation. Moreover, in both cases, the percolation has identified some anode side voxels (at Thickness=0) as parts of cracks. This is directly related to the constraint on the investigation box, where voxels on the box dark faces (Figure 4) are excluded from the boundary voxels (the initial investigation box is larger than the width). Hence, the algorithm is unable to stop the percolation at this location during the first phase of the percolation process. Reducing the initial investigation box would decrease the crack detection performance [4]. This could be avoided by increasing the anode volume investigated, e.g. anode slice of 200 to 300 mm thick or eventually on a full anode

block. Alternatively, decreasing the sphericity threshold (e.g. $\Psi = 0.25$) could have help to eliminate the "side voxels" but this did not improved significantly the detection result.

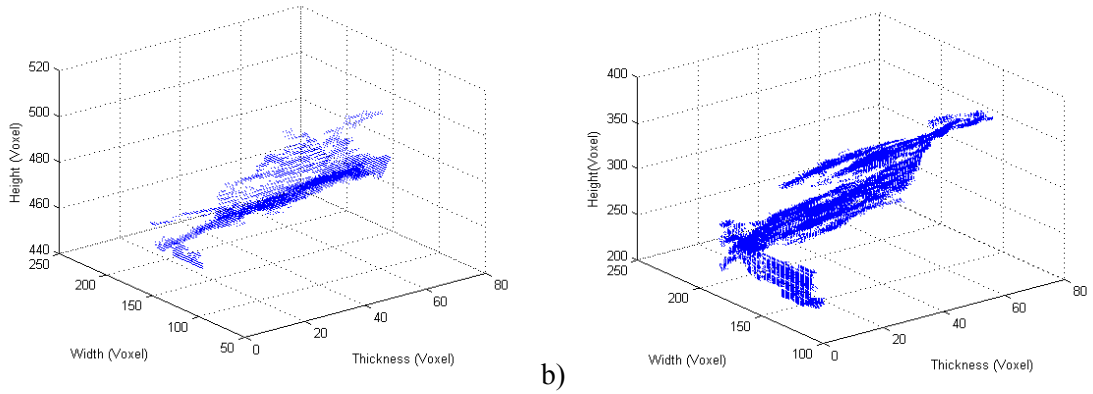

a) b)

Figure 10 Cracks detection results with restriction on the investigation box ($\Psi = 0.5$). a) Seed voxel #1. b) Seed voxel #2.

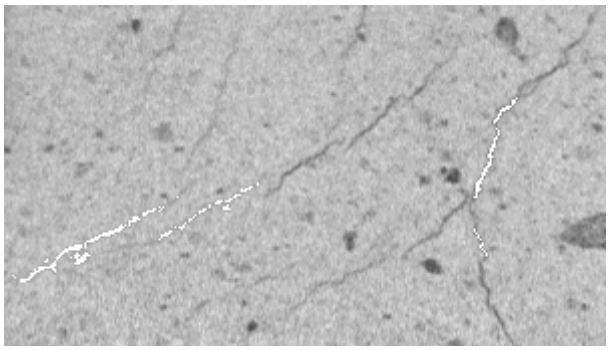

Figure 11 Cracks detection results (white regions) with restriction on the investigation box. Image located at mid width of the anode slice. Left crack: near stub hole. Right crack: near anode slot.

4. Conclusion

A 3D crack detection tool, based on a percolation method, has been developed as a non-destructive quantification technique for baked carbon anode. The proposed algorithm is a direct extension of a 2D percolation one previously adapted for low resolution images. The development of the algorithm required the proposal of an adaptive investigation box taking into account the main features of the cracks of interest and the percolated volume sphericity was used as the threshold criterion for crack identification. The performance of the proposed 3D algorithm has been tested on a 3D partial volume of baked carbon anode (anode slice) obtained with a CT scan analysis. The results have shown the necessity of the adaptive investigation box as well as its limitation. Parts of the investigated cracks were also missed by the 3D detection tool. Nevertheless, the algorithm is very promising to quantify the cracks and thus improve the acoustic emission (AE) signals analysis for the development of a rapid and non-destructive method for quality control of baked anodes. To do so, acoustic response is currently used on the same anode slices in order to develop the method [13]. The anode response was analyzed using signal processing combined with multivariate statistical methods. The work done so far has highlighted the influence of cracks concentration on the acoustic emission (AE) signals. This result was based on 2D image observations. Hence, the 3D crack detection tools will allow a quantification of the correlation between AE signals and cracks. Future work should focus on

testing the algorithm on different CT scan resolutions and sample sizes as well as optimizing the processing time.

Acknowledgments

Authors would like to acknowledge the financial support of Natural Sciences and Engineering Research Council (NSERC) and Alcoa. A part of the research presented in this paper was financed by the Fonds de Recherche du Québec-Nature et Technologie (FRQ-NT) by the intermediary of the Aluminium Research Centre-REGAL. Particular thankfulness is dedicated to Hugues Ferland, from the REGAL group, at Laval University and to Louis-Frédéric Daigle, from INRS-ETE, for their technical support.

5. References

1. Keller, F. and P.O. Sulger, *Anode Baking*. R&D Carbon Ltd.
2. Picard, D., et al. *Characterization of prebaked carbon anode samples using X-ray computed tomography and porosity estimation*. in *Light Metals 2012 - TMS 2012 Annual Meeting and Exhibition, March 11, 2012 - March 15, 2012*. 2012. Orlando, FL, United states: Minerals, Metals and Materials Society.
3. Picard, D., et al., *Characterization of a full-scale prebaked carbon anode using X-ray computerized tomography.* Light Metals 2011, 2011: p. 973-978.
4. Picard, D., et al. *Automated crack detection method applied to CT images of baked carbon anode*. in *Light Metals 2014 - TMS 2014 Annual Meeting and Exhibition, February 16, 2014 - February 20, 2014*. 2014. San Diego, CA, United states: Minerals, Metals and Materials Society.
5. Yamaguchi, T. and S. Hashimoto, *Fast crack detection method for large-size concrete surface images using percolation-based image processing.* Mach. Vision Appl., 2010. **21**(5): p. 797-809.
6. Paetsch, O., et al. *Automated 3D Crack Detection for Analyzing Damage Processes in Concrete with Computed Tomography*. in *iCT2012 - Conference on Industrial Computed Tomography* 2012. University of Applied Sciences, Upper Austria.
7. Roseman, A.M., *Particle finding in electron micrographs using a fast local correlation algorithm.* Ultramicroscopy, 2003. **94**(3-4): p. 225-236.
8. Yamaguchi, T. and S. Hashimoto. *Automated Crack Detection for Concrete Surface Image Using Percolation Model and Edge Information*. in *IEEE Industrial Electronics, IECON 2006 - 32nd Annual Conference on*. 2006.
9. Yamaguchi, T. and S. Hashimoto, *Image Processing Based on Percolation Model.* IEICE - Trans. Inf. Syst., 2006. **E89-D**(7): p. 2044-2052.
10. Yamaguchi, T., S. Nakamura, and S. Hashimoto. *An efficient crack detection method using percolation-based image processing*. in *Industrial Electronics and Applications, 2008. ICIEA 2008. 3rd IEEE Conference on*. 2008.
11. Heimann, T. and H.P. Meinzer, *Statistical shape models for 3D medical image segmentation: a review.* Medical Image Analysis, 2009. **13**(4): p. 543-63.
12. Legland, D., K. Kieu, and M.-F. Devaux, *Computation of Minkowski measures on 2D and 3D binary images.* Image Analysis and Stereology, 2007. **26**(2): p. 83-92.
13. Ben Boubaker, M., et al. *Inspection of baked carbon anodes using acoustic techniques*. in *ICSOBA-2015*. 2015. Dubai.